ARMY RESEARCH LABORATORY

A Conformal-Mapping Treatment of the Effect of a Semi-Infinite Gate on a Two-Dimensional Electron Gas

Frank J. Crowne

ARL-TR-2153 August 2000

The findings in this report are not to be construed as an official Department of the Army position unless so designated by other authorized documents.

Citation of manufacturer's or trade names does not constitute an official endorsement or approval of the use thereof.

Destroy this report when it is no longer needed. Do not return it to the originator.

Army Research Laboratory

Adelphi, MD 20783-1197

ARL-TR-2153 **August 2000**

A Conformal-Mapping Treatment of the Effect of a Semi-Infinite Gate on a Two-Dimensional Electron Gas

Frank J. Crowne

Sensors and Electron Devices Directorate

Abstract

A pinched-off high-electron-mobility transistor containing a perfectly conducting two-dimensional electron gas (2DEG) is described mathematically within an idealized two-dimensional geometry, so that conformal mapping techniques can be used to compute internal fields at the transistor drain. The field and charge distribution at the drain end of the 2DEG calculated in this way suggest that the charge is a nonmonotonic function of position in this region.

Contents

Figures

1. Introduction

The physics of field-effect transistors (FETs) fundamentally differs from that of bipolar transistors and heterojunction-bipolar transistors (HBTs), in which currents flow perpendicular to layers of various materials. This difference arises from the lateral geometry that underlies the operation of FETs, i.e., the modulation of a "horizontal" current that arises from a drain-to-source voltage by "vertical" electric fields generated by a gate electrode. The FET geometry gives rise to internal electric fields that are complicated and intrinsically two-dimensional (2D), so that the device terminal characteristics (source, drain, and gate voltages and currents) become difficult to predict and dependent on many internal parameters. The geometry makes the physics of 2D electron-gas (2DEG) FETs (high-electron-mobility transistors—HEMTs) especially difficult to unravel, since the quantum-mechanical nature of the electron dynamics in the 2D channel cannot easily be disentangled from the electrostatic problem of finding the fields in the neighboring dielectric materials.

A problem of particular interest to device designers is to determine what happens to the 2DEG as it emerges from under the gate region. Because the electric fields are no longer screened by the gate, the capacitance of the electron gas per unit length with respect to the gate must change, since field lines can now escape to infinity. This problem is made even more interesting by the existence of plasma oscillations predicted by Dyakonov and Shur in 1993 [1], which are profoundly different for a gated and an ungated electron gas [2]. In this report, conformal mapping is used to compute the change in field configuration of the electron gas in this situation, with the extreme assumption of a perfectly conducting electron gas. The finite-conductivity effects needed for the study of plasma oscillations will be the subject of a subsequent report.

Figure 1 is a cross section of the device geometry near the drain. The 2DEG is assumed to be a vertical distance h below the gate and to terminate at a horizontal distance q beyond the drain end of the gate. Let us begin with the symmetrized version of this geometry shown in figure 2 (resembling that of a junction FET (JFET) [3]) and tailored for a treatment based on complex-variable theory. The new geometry, which is embedded in the complex plane $z = x + iy$, has the following idealized features:

1. There are two gates separated by a distance h, with the 2DEG between them along the $x = \mathrm{Re}\, z$ axis and ending at a point $x = q > 0$ on the real axis.
2. The 2DEG is infinitely extended to the left.
3. The gates are both assumed to be infinitely thick, with vertical boundaries along the $y = \mathrm{Im}\, z$-axis.

4. All dielectric constants are set equal to one.

This idealized geometry will allow us to set up the conformal-mapping problem discussed in the next section.

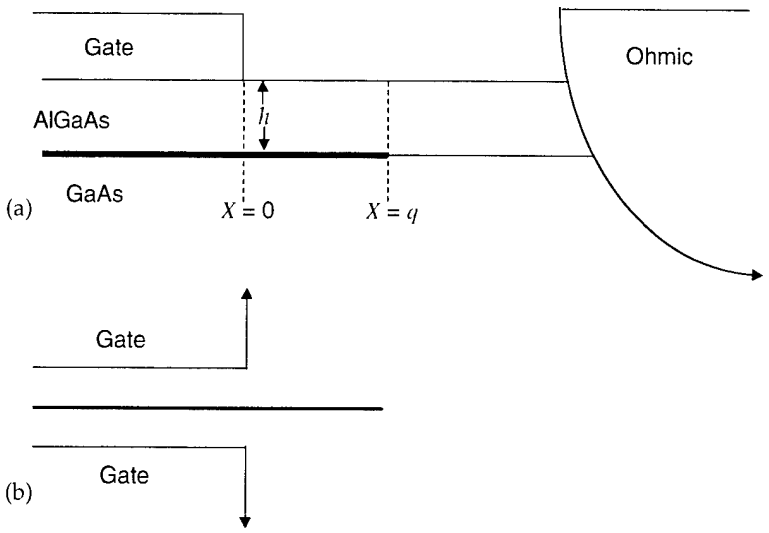

Figure 1. Cross section of FET geometry on drain side of 2DEF FET: (a) real and (b) idealized.

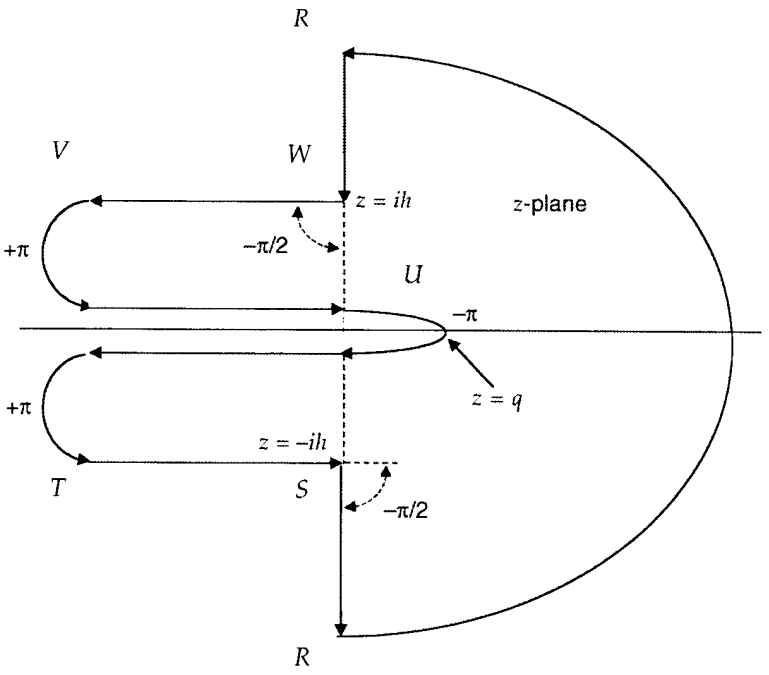

Figure 2. Physical (z) plane for Schwartz-Christoffel mapping.

2. Schwartz-Christoffel Transformation

Following standard procedures [4], I seek a complex-variable function that will map the shaded area in figure 2 (the z-plane) into the upper half of a new complex-variable plane, the w-plane. The special points $R, S, T, U, V,$ and W identify the right-hand half-space (R), the lower gate edge (S), points deep inside the gated channel and below the 2DEG (T), the end of the 2DEG (U), points deep inside the gated channel and above the 2DEG (V), and the upper gate edge (W). The Schwartz-Christoffel recipe treats this geometry as a seven-sided polygon with the point R at infinity. Because of the symmetry, we can assume that the points in the complex z-plane other than R pair symmetrically in the w-plane; this results in the following differential equation for the Schwartz-Christoffel mapping:

$$\frac{dz}{dw} = A\frac{w\sqrt{w^2 - c^2}}{w^2 - 1}, \tag{1}$$

where A and c are to be determined. The function $w(z)$ maps the points $R, S, T, U, V,$ and W in the z-plane into the points in figure 3 on the real axis of the complex w-plane. The problem now reduces to

1. solving this equation,
2. finding values of A and c,
3. solving the Laplace equation in the w-plane, and
4. inverting the transformation to return to the z-plane.

Figure 4 shows the proper definition of the branch cuts for the function $\sqrt{w^2 - c^2}$: $\arg(w - c) \in [-\pi, \pi], \arg(w + c) \in [-\pi, \pi]$.

Figure 3. Schwartz-Christoffel plane.

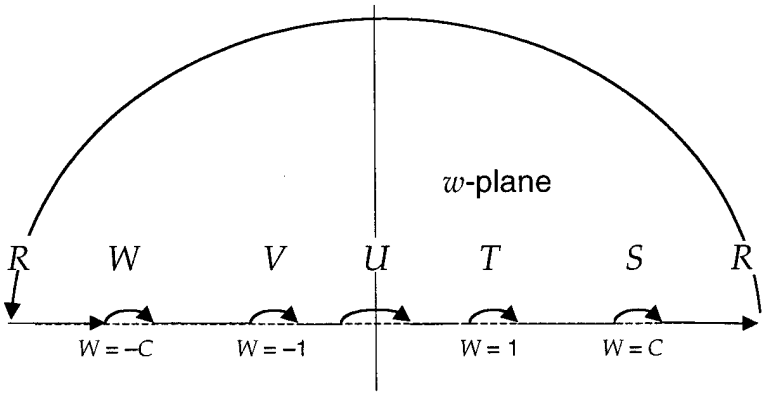

Figure 4. Branch cuts for $w(z)$.

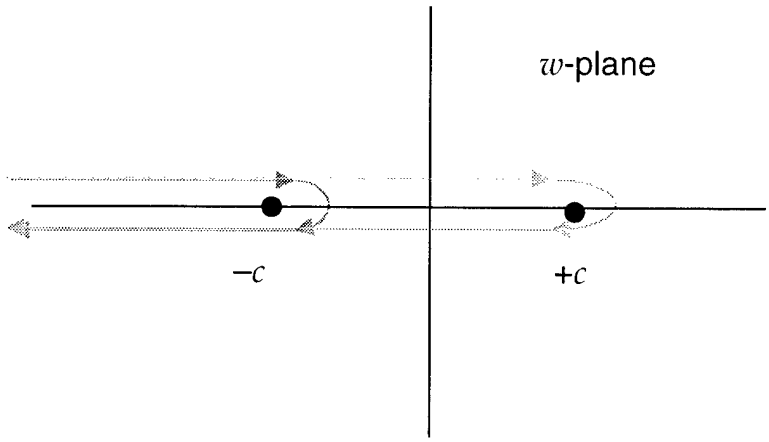

The differential equation is trivially solved for the function $z(w)$:

$$z(w) = z_0 + A\int_c^w \frac{\sqrt{\xi^2 - c^2}}{\xi^2 - 1}\xi\, d\xi = z_0 + A\left[\sqrt{\frac{w^2 - c^2}{c^2 - 1}} - \tan^{-1}\sqrt{\frac{w^2 - c^2}{c^2 - 1}}\right], \tag{2}$$

which we can rewrite as

$$z(w) = z_0 + A\left[\sqrt{\frac{w^2 - c^2}{c^2 - 1}} - \frac{1}{2i}\ln\left\{\frac{1 + i\sqrt{\frac{w^2-c^2}{c^2-1}}}{1 - i\sqrt{\frac{w^2-c^2}{c^2-1}}}\right\}\right]. \tag{3}$$

Now, consider the action of this mapping from various regions of $\mathrm{Re}\, w$ to the z-plane:

1. $w \in [-\infty, -c]$ (segment RW): for large w, $z \approx z_0 + A\frac{w}{\sqrt{c^2-1}} \to +i\infty$, so that $A = iB$ with $B < 0$. As $w \to c$, the term in brackets vanishes; since $w = c$ must correspond to $z = +ih$ in the physical z-plane, we have $z_0 = ih$. Then

$$z = ih + iB\left[\sqrt{\frac{w^2 - c^2}{c^2 - 1}} - \tan^{-1}\sqrt{\frac{w^2 - c^2}{c^2 - 1}}\right]. \tag{4}$$

2. $w \in [-c, -1]$ (segment WV): On this segment of $\mathrm{Re}\, w$, we have $\sqrt{\frac{w^2-c^2}{c^2-1}} = i\sqrt{\frac{c^2-w^2}{c^2-1}}$, with $\sqrt{\frac{c^2-w^2}{c^2-1}} < 1$, according to our choice of branch cut, so we can rewrite $z(w)$ as

$$\begin{aligned} z &= ih + iB\left[i\sqrt{\frac{c^2 - w^2}{c^2 - 1}} - \frac{1}{2i}\ln\left\{\frac{1 - \sqrt{\frac{c^2-w^2}{c^2-1}}}{1 + \sqrt{\frac{c^2-w^2}{c^2-1}}}\right\}\right] \\ &= ih - B\left[\sqrt{\frac{c^2 - w^2}{c^2 - 1}} - \frac{1}{2}\ln\left\{\frac{1 + \sqrt{\frac{c^2-w^2}{c^2-1}}}{1 - \sqrt{\frac{c^2-w^2}{c^2-1}}}\right\}\right] \\ &= ih - B\left[\sqrt{\frac{c^2 - w^2}{c^2 - 1}} - \tanh^{-1}\sqrt{\frac{c^2 - w^2}{c^2 - 1}}\right]. \end{aligned} \tag{5}$$

From this we see that $w \to -1 \Rightarrow z \to ih - \infty$, so long as $B < 0$ and real. This takes care of segment WV.

3. $w \in [-1, 0]$ (segment VU): On this segment of $\mathrm{Re}\, w$, we have $\sqrt{\frac{c^2-w^2}{c^2-1}} > 1$, so that the hyperbolic tangent is affected. Write

$$\frac{1}{2}\ln\left\{\frac{1+\sqrt{\frac{c^2-w^2}{c^2-1}}}{1-\sqrt{\frac{c^2-w^2}{c^2-1}}}\right\} = \frac{1}{2}\ln\left\{\frac{\sqrt{\frac{c^2-w^2}{c^2-1}}+1}{(-1)\left(\sqrt{\frac{c^2-w^2}{c^2-1}}-1\right)}\right\} \tag{6}$$

and pick the log branch cut such that $\ln(-x) = -i\pi + \ln(x)$. Then

$$z = \frac{1}{2}\ln\left\{\frac{1+\sqrt{\frac{c^2-1}{c^2-w^2}}}{1-\sqrt{\frac{c^2-1}{c^2-w^2}}}\right\} + \frac{i\pi}{2} = \tanh^{-1}\left(\sqrt{\frac{c^2-1}{c^2-w^2}}\right) + \frac{i\pi}{2} \tag{7}$$

and so

$$z = ih - B\left[\sqrt{\frac{c^2-w^2}{c^2-1}} - \tanh^{-1}\left(\sqrt{\frac{c^2-1}{c^2-w^2}}\right) - \frac{i\pi}{2}\right]. \tag{8}$$

Now, let us choose the point $z = q$, where q is real, to correspond to $w = 0$. This will be true if $B = -\frac{2h}{\pi}$ and

$$q = \frac{2h}{\pi}\left[\frac{c}{\sqrt{c^2-1}} - \tanh^{-1}\left(\sqrt{\frac{c^2-1}{c}}\right)\right]. \tag{9}$$

This equation now determines c in terms of the real parameter q. Then

$$z = \frac{2h}{\pi}\left[\sqrt{\frac{c^2-w^2}{c^2-1}} - \tanh^{-1}\left(\sqrt{\frac{c^2-1}{c^2-w^2}}\right)\right] \tag{10}$$

and $w \to -1 \Rightarrow z \to -\infty$ (from the inverse hyperbolic tangent), while $w \to 0 \Rightarrow z \to q$.

Let $x = \frac{\sqrt{c^2-1}}{c}$. Then equation (9) becomes

$$\frac{1}{x} - \frac{\pi q}{2h} = \tanh^{-1}(x). \tag{11}$$

The plot in figure 5 shows that there is an acceptable root x for every $q \in [-\infty, \infty]$, where the root x is always in the range $[0, 1]$.

4. $w \in [0, 1]$ (segment UT): This is the same as $w \in [-1, 0]$, since the function depends on w^2, but it runs backwards, and $w \to 1 \Rightarrow z \to -\infty, w \to 0 \Rightarrow z \to q$ once more.

5. $w \in [1, c]$ (segment TS): Here we have

$$z = \frac{2h}{\pi}\left[\sqrt{\frac{c^2-w^2}{c^2-1}} - \tanh^{-1}\left(\sqrt{\frac{c^2-1}{c^2-w^2}}\right)\right]. \tag{12}$$

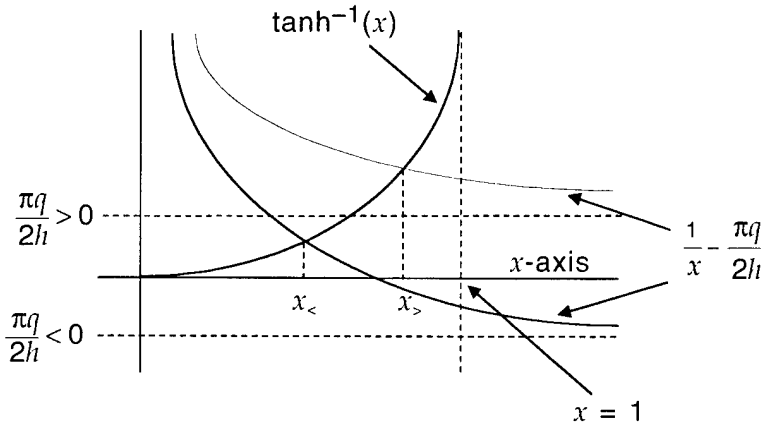

Figure 5. Graphical solution to equation for c, which locates mapping point q that terminates 2DEG; $x_>$ is root for $\pi q/2h > 0$, and $x_<$ is root for $\pi q/2h < 0$.

Since $w > 1 \Rightarrow \sqrt{\frac{c^2-1}{c^2-w^2}} > 1$, we have

$$\begin{aligned} -\tanh^{-1}\left(\sqrt{\frac{c^2-1}{c^2-w^2}}\right) &= -\frac{1}{2}\ln\left\{\frac{1+\sqrt{\frac{c^2-1}{c^2-w^2}}}{1-\sqrt{\frac{c^2-1}{c^2-w^2}}}\right\} \\ &= \frac{1}{2}\ln\left\{\frac{(-1)\left(\sqrt{\frac{c^2-1}{c^2-w^2}}-1\right)}{\sqrt{\frac{c^2-1}{c^2-w^2}}+1}\right\} \\ &= \frac{1}{2}\ln\left\{\frac{1-\sqrt{\frac{c^2-w^2}{c^2-1}}}{1+\sqrt{\frac{c^2-w^2}{c^2-1}}}\right\} - \frac{i\pi}{2} \\ &= -\tanh^{-1}\left(\sqrt{\frac{c^2-w^2}{c^2-1}}\right) - \frac{i\pi}{2}. \end{aligned} \quad (13)$$

Then

$$\begin{aligned} z &= \frac{2h}{\pi}\left[\sqrt{\frac{c^2-w^2}{c^2-1}} - \tanh^{-1}\left(\sqrt{\frac{c^2-w^2}{c^2-1}}\right) - \frac{i\pi}{2}\right] \\ &= -ih + \frac{2h}{\pi}\left[\sqrt{\frac{c^2-w^2}{c^2-1}} - \tanh^{-1}\left(\sqrt{\frac{c^2-w^2}{c^2-1}}\right)\right] \end{aligned} \quad (14)$$

on this segment. Note that $w \to 1 \Rightarrow z \to -ih - \infty$, as it should.

6. $w \in [c, \infty]$ (segment SR): On this segment we have $\sqrt{\frac{c^2-w^2}{c^2-1}} = -i\sqrt{\frac{w^2-c^2}{c^2-1}}$, so that

$$\begin{aligned} \tanh^{-1}\left(-i\sqrt{\frac{w^2-c^2}{c^2-1}}\right) &= \frac{1}{2}\ln\left(\frac{1-i\sqrt{\frac{w^2-c^2}{c^2-1}}}{1+i\sqrt{\frac{w^2-c^2}{c^2-1}}}\right) \\ &= -\frac{1}{2}\ln\left(\frac{1+i\sqrt{\frac{w^2-c^2}{c^2-1}}}{1-i\sqrt{\frac{w^2-c^2}{c^2-1}}}\right) \end{aligned}$$

$$= -i\,\frac{1}{2i}\ln\left(\frac{1+i\sqrt{\frac{w^2-c^2}{c^2-1}}}{1-i\sqrt{\frac{w^2-c^2}{c^2-1}}}\right)$$

$$= -i\tan^{-1}\left(\sqrt{\frac{w^2-c^2}{c^2-1}}\right) \qquad (15)$$

and

$$z = -ih + \frac{2h}{\pi}\left[-i\sqrt{\frac{w^2-c^2}{c^2-1}} + i\tan^{-1}\left(\sqrt{\frac{w^2-c^2}{c^2-1}}\right)\right]$$

$$= -ih - \frac{2ih}{\pi}\left[\sqrt{\frac{w^2-c^2}{c^2-1}} - \tan^{-1}\left(\sqrt{\frac{w^2-c^2}{c^2-1}}\right)\right]. \qquad (16)$$

Clearly, for large real $w > 0$, we have $z \approx -ih - \frac{2ih}{\pi}\frac{w}{\sqrt{c^2-1}} \to -i\infty$, which is physically correct. Note that the Schwartz reflection principle implies that if $w = u + iv$ and z is a function of w^2, then

$$z(\{-u+iv\}^2) = z(\{w^*\}^2) = z(\{w^2\}^*) = z^*(w^2). \qquad (17)$$

Hence, moving to $\mathrm{Re}\,w < 0$ in the upper half of the w-plane takes you to the lower half of the z-plane.

3. Perfectly Conducting 2DEG

Here $V = 0$ on the electrodes, and $V = V_0$ on the 2DEG between them. Then the complex potential is

$$V(z) = \frac{V_0}{\pi}\mathrm{Im}\left\{\ln\left(\frac{w(z)-1}{w(z)+1}\right)\right\} \equiv \mathrm{Im}\, U(w(z)). \tag{18}$$

which reproduces the expression given in Churchill and Brown [5]. The electric field components are

$$E_x = \frac{\partial V}{\partial x} = \mathrm{Im}\left[\frac{\partial U}{\partial x}\right] = \mathrm{Im}\left[\frac{\partial U}{\partial z}\right] = \mathrm{Im}\left[U'(w)w'(z)\right] \tag{19}$$

and

$$E_y = \frac{\partial V}{\partial y} = \mathrm{Im}\left[\frac{\partial U}{\partial y}\right] = \mathrm{Im}\left[i\frac{\partial U}{\partial z}\right] = \mathrm{Re}\left[U'(w)w'(z)\right]. \tag{20}$$

But

$$\frac{dw}{dz} = \left\{\frac{dz}{dw}\right\}^{-1} = \frac{i\pi}{2h}\,\frac{w^2-1}{w\sqrt{w^2-c^2}} \tag{21}$$

and

$$\frac{\partial U}{\partial z} = \frac{2V_0}{\pi}\,\frac{1}{w^2-1}, \tag{22}$$

so that

$$\begin{aligned} U'(w)w'(z) &= \frac{2V_0}{\pi}\,\frac{1}{w^2-1}\,\frac{i\pi}{2h}\,\frac{w^2-1}{w\sqrt{w^2-c^2}} \\ &= \frac{iV_0}{h}\,\frac{1}{w\sqrt{w^2-c^2}}. \end{aligned} \tag{23}$$

Since $|w| < c$ everywhere on the z-axis, we can write

$$\begin{aligned} E_x &= \frac{V_0}{h}\,\mathrm{Im}\frac{1}{w\sqrt{c^2-w^2}}, \\ E_y &= \frac{V_0}{h}\,\mathrm{Re}\frac{1}{w\sqrt{c^2-w^2}}, \quad \text{and} \\ |E| &= \frac{V_0}{h}\left|\frac{1}{w\sqrt{c^2-w^2}}\right|. \end{aligned} \tag{24}$$

A few things to note:

1. $E_x = 0$ for real w; i.e., the vector E is normal to the $\mathrm{Re}\, z$ axis, as it should be for a perfect conductor.
2. The field has a $|z|^{-1/2}$ singularity at the end of the 2DEG.
3. The field has $|c \pm z|^{-1/3}$ singularities at the electrode corners.

4. At large z, $\mathrm{Re}\, z > 0$ (or large w, $\mathrm{Re}\, w > 0$), the field goes as $|z|^{-2}$, i.e., like a dipole. Hence, the electrode charges completely screen out the 2DEG charge at large distances.

5. For large z, $\mathrm{Re}\, z < 0$, and $\mathrm{Im}\, z[-ih, ih]$ (or $w \to \pm 1$), the field approaches a constant:

$$E_y = \pm \frac{V_0}{h} \frac{1}{\sqrt{c(q)^2 - 1}}, \tag{25}$$

where the sign is the same as that of $\mathrm{Im} z$. This is also correct, since the problem is x-independent in this limit. Since $C = \frac{Q}{V_0}$ and $Q = 2E_y$ by Gauss's law, we obtain the following nontrivial fringing capacitance/length,

$$C = \frac{2\epsilon}{h} \frac{1}{\sqrt{c(q)^2 - 1}}, \tag{26}$$

associated with the termination of the gate.

Figure 6 shows a numerical calculation of the 2D density of a perfectly conducting 2DEG using the expressions derived in this report and the parameter values $q = 4$, $h = 1$ (only their ratio enters in, so the units are arbitrary). Note that in a plasma-active device structure, the potential and density would be coupled in a complicated way, with both acting as degrees of freedom, rather than having the potential as a constant. Despite the oversimplification, however, the variation of the 2DEG density is highly nontrivial, with a minimum about 80 percent of the way to the end of the gas. This is presumably because the image fields from the sharp corners are trying to hold the electrons within the region between the electrodes, which competes with their natural tendency to accumulate at the end of the gas. The fringing capacitance here is about 12.6 ϵ/h for this geometry.

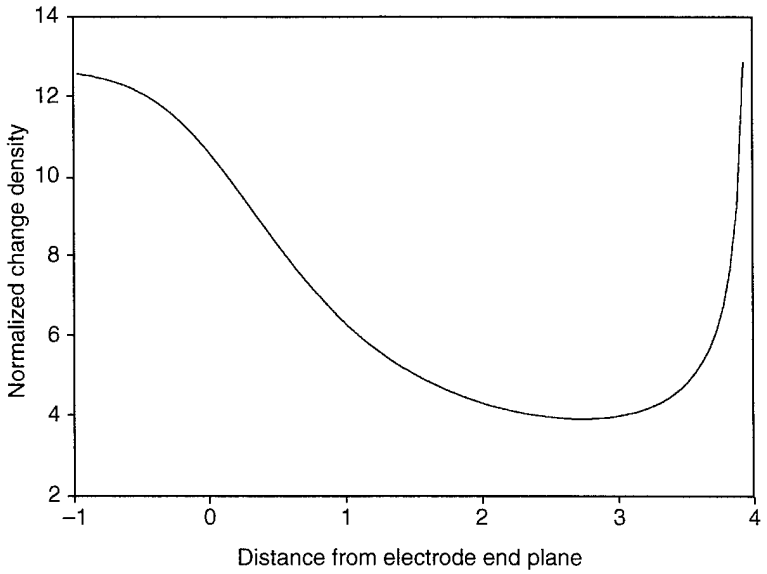

Figure 6. Density distribution of perfectly conducting 2DEG. Note divergence at endpoint ($z = 4$).

4. Conclusions

The predicted form of the charge density near the end of the gate suggests that plasma oscillations that propagate to this point will see a depletion region. This corresponds to a region of decreased Dyakonov-Shur plasma velocity, which in turn suggests that plasma waves will see an impedance mismatch between the gated and ungated regions over and above what would be expected from their intrinsic dissimilarity. Because the central assumption of the Dyakonov-Shur plasma model of a 2DEG FET is a special set of boundary conditions at the gate and source, the existence of this "natural" boundary condition may require that their assumptions be reexamined, and could perhaps explain why plasma oscillations have yet to be observed in standard HEMTs.

References

1. M. Dyakonov and M. Shur, "Shallow Water Analogy for a Ballistic Field Effect Transistor: New Mechanism of Plasma Wave Generation by dc Current," *Phys. Rev. Lett.* **71** (1993), 2465.

2. F. Crowne, "Contact Boundary Conditions and the Dyakonov-Shur Instability in High Electron Mobility Transistors," *J. Appl. Phys.* **82** (1997), 1242.

3. S. M. Sze, *Physics of Semiconductor Devices*, Wiley & Sons, New York (1981), ch 6.

4. G. F. Carrier, M. Krook, and C. E. Pearson, *Functions of a Complex Variable*, McGraw-Hill, New York (1966), §4-4.

5. R. V. Churchill and J. W. Brown, *Complex Variables and Applications*, McGraw-Hill Series in Higher Mathematics, McGraw-Hill, New York (1989), p 237.

Distribution

Admnstr
Defns Techl Info Ctr
Attn DTIC-OCP
8725 John J Kingman Rd Ste 0944
FT Belvoir VA 22060-6218

Ofc of the Secy of Defns
Attn ODDRE (R&AT)
The Pentagon
Washington DC 20301-3080

Ofc of the Secy of Defns
Attn OUSD(A&T)/ODDR&E(R) R J Trew
3080 Defense Pentagon
Washington DC 20301-7100

AMCOM MRDEC
Attn AMSMI-RD W C McCorkle
Redstone Arsenal AL 35898-5240

CECOM
Attn PM GPS COL S Young
FT Monmouth NJ 07703

DARPA
Attn DARPA/MTO E Martinez
3701 N Fairfax Dr
Arlington VA 22203-1714

Dir for MANPRINT
Ofc of the Deputy Chief of Staff for Prsnnl
Attn J Hiller
The Pentagon Rm 2C733
Washington DC 20301-0300

US Army ARDEC
Attn AMSTA-AR-TD M Fisette
Bldg 1
Picatinny Arsenal NJ 07806-5000

US Army Info Sys Engrg Cmnd
Attn ASQB-OTD F Jenia
FT Huachuca AZ 85613-5300

US Army Natick RDEC Acting Techl Dir
Attn SSCNC-T P Brandler
Natick MA 01760-5002

US Army Simulation, Train, & Instrmntn Cmnd
Attn J Stahl
12350 Research Parkway
Orlando FL 32826-3726

US Army Soldier & Biol Chem Cmnd Dir of Rsrch & Techlgy Dirctrt
Attn SMCCR-RS I G Resnick
Aberdeen Proving Ground MD 21010-5423

US Army Tank-Automtv Cmnd Rsrch, Dev, & Engrg Ctr
Attn AMSTA-TR J Chapin
Warren MI 48397-5000

US Army Train & Doctrine Cmnd
Battle Lab Integration & Techl Dirctrt
Attn ATCD-B J A Klevecz
FT Monroe VA 23651-5850

US Military Academy
Mathematical Sci Ctr of Excellence
Attn MDN-A LTC M D Phillips
Dept of Mathematical Sci Thayer Hall
West Point NY 10996-1786

Nav Surface Warfare Ctr
Attn Code B07 J Pennella
17320 Dahlgren Rd Bldg 1470 Rm 1101
Dahlgren VA 22448-5100

DARPA
Attn S Welby
3701 N Fairfax Dr
Arlington VA 22203-1714

Univ of Maryland Lab for Physical Sci
Attn K Ritter
Attn W Beard
College Park MD 20742

Hicks & Associates Inc
Attn G Singley III
1710 Goodrich Dr Ste 1300
McLean VA 22102

Distribution(cont'd)

Palisades Inst for Rsrch Svc Inc
Attn E Carr
1745 Jefferson Davis Hwy Ste 500
Arlington VA 22202-3402

US Army Rsrch Lab
Attn AMSRL-SL-BN J Soln
Aberdeen Proving Ground MD 21005

Director
US Army Rsrch Ofc
Attn H Everitt
Attn AMSRL-RO M Stroscio
Attn D Wolard
Attn J Harvey
Attn J Prater
Attn M Dutta
Attn AMSRL-RO-D JCI Chang
PO Box 12211
Research Triangle Park NC 27709

US Army Rsrch Lab
Attn AMSRL-DD J M Miller
Attn AMSRL-CI-AI-R Mail & Records Mgmt
Attn AMSRL-CI-AP Techl Pub (3 copies)
Attn AMSRL-CI-LL Techl Lib (3 copies)
Attn AMSRL-SE E Poindexter
Attn AMSRL-SE J M McGarrity
Attn AMSRL-SE J Pellegrino
Attn AMSRL-SE-DP A Bromborsky
Attn AMSRL-SE-DP H Brandt
Attn AMSRL-SE-DP R del Rosario
Attn AMSRL-SE-DS C Fazi
Attn AMSRL-SE-E H Pollehn
Attn AMSRL-SE-E J Mait
Attn AMSRL-SE-E W Clark
Attn AMSRL-SE-EE A Goldberg
Attn AMSRL-SE-EE D Beekman
Attn AMSRL-SE-EE M Patterson

US Army Rsrch Lab (cont'd)
Attn AMSRL-SE-EE S Kennerly
Attn AMSRL-SE-EE Z G Sztankay
Attn AMSRL-SE-EI B Beck
Attn AMSRL-SE-EI J Little
Attn AMSRL-SE-EI K K Choi
Attn AMSRL-SE-EI M Tidrow
Attn AMSRL-SE-EI N Dhar
Attn AMSRL-SE-EI R Leavitt
Attn AMSRL-SE-EI T Zheleva
Attn AMSRL-SE-EM G Simonis
Attn AMSRL-SE-EM J Pamulapati
Attn AMSRL-SE-EM M Tobin
Attn AMSRL-SE-EM P Shen
Attn AMSRL-SE-EM W Chang
Attn AMSRL-SE-EO N Gupta
Attn AMSRL-SE-EP D Wortman
Attn AMSRL-SE-EP J Bradshaw
Attn AMSRL-SE-EP J Bruno
Attn AMSRL-SE-EP M Wraback
Attn AMSRL-SE-EP P Folkes
Attn AMSRL-SE-EP R Tober
Attn AMSRL-SE-EP S Rudin
Attn AMSRL-SE-EP T B Bahder
Attn AMSRL-SE-EP T Oldham
Attn AMSRL-SE-R B Wallace
Attn AMSRL-SE-RE F Crowne (5 copies)
Attn AMSRL-SE-RE R Chase
Attn AMSRL-SE-RE R Kaul
Attn AMSRL-SE-RE S Tidrow
Attn AMSRL-SE-RL C Scozzie
Attn AMSRL-SE-RL A Lepore
Attn AMSRL-SE-RL M Dubey
Attn AMSRL-SE-RL S Svensson
Attn AMSRL-SE-SS K Jones
Adelphi MD 20783-1197

REPORT DOCUMENTATION PAGE

Form Approved
OMB No. 0704-0188

1. AGENCY USE ONLY *(Leave blank)*	2. REPORT DATE	3. REPORT TYPE AND DATES COVERED
	August 2000	Interim, 6/99–12/99

4. TITLE AND SUBTITLE A Conformal-Mapping Treatment of the Effect of a Semi-Infinite Gate on a Two-Dimensional Electron Gas

5. FUNDING NUMBERS
DA PR: AH94
PE: 62120.A

6. AUTHOR(S) Frank J. Crowne

7. PERFORMING ORGANIZATION NAME(S) AND ADDRESS(ES)
U.S. Army Research Laboratory
Attn: AMSRL-SE-RE email: fcrowne@arl.mil
2800 Powder Mill Road
Adelphi, MD 20783-1197

8. PERFORMING ORGANIZATION REPORT NUMBER
ARL-TR-2153

9. SPONSORING/MONITORING AGENCY NAME(S) AND ADDRESS(ES)
U.S. Army Research Laboratory
2800 Powder Mill Road
Adelphi, MD 20783-1197

10. SPONSORING/MONITORING AGENCY REPORT NUMBER

11. SUPPLEMENTARY NOTES
ARL PR: ONE6K1
AMS code: 622705.H94

12a. DISTRIBUTION/AVAILABILITY STATEMENT Approved for public release; distribution unlimited.

12b. DISTRIBUTION CODE

13. ABSTRACT *(Maximum 200 words)*
A pinched-off high-electron-mobility transistor containing a perfectly conducting two-dimensional electron gas (2DEG) is described mathematically within an idealized two-dimensional geometry, so that conformal mapping techniques can be used to compute internal fields at the transistor drain. The field and charge distribution at the drain end of the 2DEG calculated in this way suggest that the charge is a nonmonotonic function of position in this region.

14. SUBJECT TERMS Conformal mapping, two-dimensional electron gas

15. NUMBER OF PAGES 19

16. PRICE CODE

17. SECURITY CLASSIFICATION OF REPORT	18. SECURITY CLASSIFICATION OF THIS PAGE	19. SECURITY CLASSIFICATION OF ABSTRACT	20. LIMITATION OF ABSTRACT
Unclassified	Unclassified	Unclassified	UL

NSN 7540-01-280-5500

Standard Form 298 (Rev. 2-89)
Prescribed by ANSI Std. Z39-18
298-102